

**RASTER IMAGE CORRELATION SPECTROSCOPY [RICS]  
ANALYSIS OF HELA CELLS**

A Thesis

by

HARINI BYTARAYA SREENIVASAPPA

Submitted to the Office of Graduate Studies of  
Texas A&M University  
in partial fulfillment of the requirements for the degree of

MASTER OF SCIENCE

December 2009

Major Subject: Electrical Engineering

# **RASTER IMAGE CORRELATION SPECTROSCOPY [RICS]**

## **ANALYSIS OF HELA CELLS**

A Thesis

by

**HARINI BYTARAYA SREENIVASAPPA**

Submitted to the Office of Graduate Studies of  
Texas A&M University  
in partial fulfillment of the requirements for the degree of

**MASTER OF SCIENCE**

Approved by:

Chair of Committee,	Jun Kameoka
Committee Members,	Chin Su
	Xing Cheng
	Kuang-An Chang
Head of Department,	Costas Georghiadis

December 2009

Major Subject: Electrical Engineering

## **ABSTRACT**

Raster Image Correlation Spectroscopy [RICS] Analysis of HeLa cells.

(December 2009)

Harini Bytaraya Sreenivasappa, BE, Atria Institute of Technology.

Chair of Advisory Committee: Dr. Jun Kameoka

The objective of the project is to use the RICS analysis technique in complement with confocal microscopy to determine the diffusion coefficient of the selectively labeled green fluorescent protein (GFP), GFP-EGFR and GFP-p53 in cervical cancer cells. This is a collaboration work with MD Anderson Cancer Center. The application of the study is to lay the foundation for further study in understanding the cell metabolism, sub-cellular morphologic and dynamic biochemical processes to aid in the diagnosis and to potentially screen cancers.

Fluorescence microscopy techniques have been developed for the study of cellular processes and molecular signal pathway. However, the spatial resolution to distinguish and resolve the interactions of single molecular complexes or molecule in cells is limited by the wavelength. Hence, indirect image correlation methods complementary to the imaging techniques were developed to obtain the dynamic information within the cell. RICS is one such mathematical image processing method to determine the dynamics of the cell.

HeLa cells are transfected with GFP to highlight the protein of interest. These samples were imaged with confocal microscope, Olympus FV1000 with a 60× 1.2 NA water objective in the pseudo photon counting mode with an excitation of 488 nm argon ion laser. About 100 frames of scan area 256×256 pixels were collected from each sample at scan speed of 12.5 seconds per pixel. The stacks of images were processed with SimFCS software. The images were subjected to immobile subtraction algorithm to remove the immobile features. Consequently, each frame in the stack is subjected to 2D-correlation; then, the average 2D-spatial correlation is calculated. This 2D-spatial correlated data constitutes as RICS data which is then displayed and analyzed by fitting it to specific models. This generates a spatial temporal map of the molecular dynamics of fluorescently labeled probes within the cell.

In summary, we apply RICS techniques based on correlation spectroscopy to the image data and quantify diffusion coefficient of protein of interest in cancerous cells with different treatments. This is expected to better understand cellular dynamics of cancerous cells and build better diagnostic biosensor devices for early screening.

## **DEDICATION**

To my parents Sreenivasappa Bytaraya and Padmavathi Sreenivasappa

## ACKNOWLEDGEMENTS

I would like to express my gratitude to my committee chair and mentor, Dr.Kameoka. He has been a guiding light from the inception to the very end. He has offered strong support and encouragement. I would also like to thank my committee members, Dr. Su, Dr. Chang, and Dr. Cheng, for their guidance and support. Thanks to Dr. Yamaguchi and Dr. Wang of M.D. Anderson for support and all the help.

I would also like to thank and recognize all my group members, Pei-Hsiang Tsou for inspiring hard work, Sungmin Hong for all the guidance and help, Nick Jing and Miao Wang for their positive encouragement and help. Thank you.

Thanks to Dr. Vitha for help with imaging, and for his patience in answering all my novice questions about imaging. Thanks also go to my friends and colleagues and the department faculty and staff for making my time at Texas A&M University a great experience. Special thanks to Tammy Carda and Jeanie Marshall for the timely advice and help with the official procedures.

Finally, thanks to my brother, Shylendra Sreenivasappa for being my moral support and also for programming an engineer's mind with biology. I am greatly indebted to my mother and father for their patience, relentless encouragement and constant never ending love. Dad thanks for the help in improving the US economy!

## NOMENCLATURE

2D	Two Dimensional
ACF	Auto Correlation Function
DNA	Deoxyribonucleic Acid
FCS	Fluorescence Correlation Spectroscopy
FRAP	Fluorescence Recovery After Photobleaching
FRET	Foster Resonance Energy Transfer
GFP	Green Fluorescent Protein
ICS	Image Correlation Spectroscopy
ICCS	Image Cross-Correlation spectroscopy
kICS	Reciprocal Space Image Correlation Spectroscopy /k-space ICS
LSM	Line Scanning Microscope
PCH	Photon Counting Histogram
PICS	Particle Image Correlation Spectroscopy
PSF	Point Spread Function
RICS	Raster Image Correlation Spectroscopy
SPT	Single Particle Tracking
STICS	Spatial Temporal Image Correlation Spectroscopy
TICS	Temporal Image Correlation Spectroscopy

## TABLE OF CONTENTS

	Page
ABSTRACT .....	iii
DEDICATION.....	v
ACKNOWLEDGEMENTS .....	vi
NOMENCLATURE .....	vii
TABLE OF CONTENTS.....	viii
LIST OF FIGURES .....	x
LIST OF TABLES.....	xi
1. INTRODUCTION .....	1
2. RICS – RASTER IMAGE CORRELATION SPECTROSCOPY .....	7
2.1 RICS-Concept .....	7
2.2 RICS-Theory.....	11
2.3 RICS-Method .....	17
2.4 Advantages of RICS Technique.....	20
3. PROTEIN STUDY .....	21
3.1 Green Fluorescent Protein - GFP .....	21
3.2 EGFR-Epidermal Growth Factor Receptor.....	22
3.3 p53 .....	23
4. MATERIALS AND METHODS.....	24
4.1 Cell Culture and Protein Transfection .....	24
4.2 Microscopy Specifications.....	24
5. RESULTS.....	26



	Page
6. DISCUSSION AND CONCLUSION.....	32
6.1 Discussion .....	32
6.2 Conclusion .....	34
6.3 Support and Recognition.....	35
REFERENCES .....	37
VITA.....	40

## LIST OF FIGURES

		Page
Figure 1	An overview of the image correlation techniques .....	4
Figure 2	RICS concept .....	9
Figure 3	Illustration of immobile subtraction in RICS .....	11
Figure 4	a) Graphical representation of autocorrelation operation, b) The spatial extent of the correlation increases due to diffusion .....	14
Figure 5	Schematic of RICS method .....	18
Figure 6	RICS method example .....	19
Figure 7	RICS analysis of GFP- EGFR in HeLa cells .....	28
Figure 8	RICS analysis of GFP- P53 without treatment in HeLa cells .....	28
Figure 9	RICS analysis of GFP- P53 with cisplatin treatment in HeLa cells .....	29
Figure 10	RICS analysis of GFP- P53 with etoposide treatment in HeLa cells .....	29
Figure 11	RICS analysis of GFP- alone with no treatment in HeLa cells .....	30
Figure 12	RICS analysis of GFP- alone with cisplatin treatment in HeLa cells .....	30
Figure 13	RICS analysis of GFP- alone with etoposide treatment in HeLa cells .....	31
Figure 14	2D spatial correlation as observed in the nucleus of the HeLa cells treated with DNA damage drugs .....	33

**LIST OF TABLES**

	Page
Table 1      Comparison of diffusion coefficients of GFP-p53 and GFP -alone in HeLa cells for different conditions.....	31

## 1. INTRODUCTION

Researchers today are focusing on learning about the underlying quantitative dynamics of the cells to develop treatment for diseases like cancer and diabetes. This need to study increasingly sophisticated problems in cellular level, at high spatial and temporal resolution has driven the development for entirely new microscopic methodologies coupled to the use of fluorescent proteins, new fluorescent dye technologies, highly sensitive detectors and inexpensive powerful algorithms for data analysis principally in the field of fluorescence microscopy. Consequently, fluorescence microscopy is an imperative tool in all fields of biological research [1].

Irrespective of development in the field of imaging techniques, achieving resolutions to study molecular level interaction has been limited by the excitation wavelength. As a result, many new techniques have been developed to provide molecular concentration, dynamics and organization at high temporal and spatial resolution. For example, single particle tracking (SPT) measures the trajectories of individual proteins or particles and determines the type of motion like brownian, directed, confined motions or anomalous diffusion. Fluorescence recovery after photobleaching (FRAP) is a photo activation approach, widely used to quantify 2D molecular diffusion and their transport between subcellular compartments. These approaches are, however, not suitable for

---

This thesis follows the style of *IEEE Transactions on NanoBioscience*.

determination of concentration, aggregation state, interactions and dynamics in different locations within the cell at different time. One of the most commonly used fluorescence technique for single molecule study is Foster Resonance Energy Transfer (FRET). FRET technique gives information about the macromolecular functional organizations at single molecular level that cannot be attained by the biochemical techniques. However, this technique does not provide information about translational diffusion [2].

In congruence, the developments in correlation optical microscopy have given the possibility to analyze several features of macromolecular dynamics for various subcellular processes. For instance, single point FCS technique observes fluorescence fluctuation in a very small volume (femto-liter scale) over a short period of time [3]. The fluctuation data collected can be subjected to both auto correlation function (ACF) analysis and photon counting histogram (PCH) analysis. In ACF, the time structure of the fluctuating signal is used to determine the characteristic diffusion coefficient and average number of molecules in the observation volume. Whereas in PCH analysis the amplitude spectrum of the fluctuating signal is used to ascertain the protein aggregation, distribution and also quantify the concentration of the labeled proteins. Stationary FCS can analyze fast dynamic processes at a single fixed spot within the cell at high temporal resolution (microsecond to millisecond time scale). On the contrary, image correlation spectroscopy (ICS), monitors dynamics of fluorescently labeled molecule for an entire image but at low temporal resolution (seconds). ICS calculates a spatial autocorrelation function from the images of laser scanning confocal microscope to

determine the number densities and aggregations state of fluorescent labeled particles. [4]. This technique is limited to extract slow dynamics due to the frame acquisition rate [5].

Recently, FCS and ICS methodologies have lead to several implementations; some of the widely used fluorescence correlation techniques include temporal ICS (TICS), spatiotemporal ICS (STICS), image cross correlation spectroscopy (ICCS), k-space ICS (kICS), raster ICS (RICS), and particle ICS (PICS). Each of these techniques have its inherent dynamic range and characteristics merits [3] and concisely represented in Fig 1.

Study of dynamic processes of the cell demands a high resolution in the time scale as a result time temporal image correlation spectroscopy analysis was introduced. TICS technique correlates an image series in time to determines the dynamics, number densities and fraction of immobile on the time scale measurements [1]. However, in TICS, dynamic processes like diffusion and flow speed are governed by factors like the number of pixels in region of analysis and number of frames in the image time series. Thus limiting TICS from measuring faster transport processes.

Spatiotemporal ICS (STICS) calculates the spatial and temporal correlation of the image series and enables determination of the direction and magnitude of the flow in the sample.

Reciprocal space image correlation spectroscopy k-space ICS (kICS) involves correlating, the spatial Fourier transforms of individual images in an image series in time [6]. It can be used to determine dynamics and number densities of fluorescently tagged membrane proteins. kICS technique is PSF-independent therefore insensitive to system errors due to blinking or bleaching of the fluorescent particles. Nevertheless, kICS analysis depends on the sample size and noise level, limiting its application in small regions of the cell.

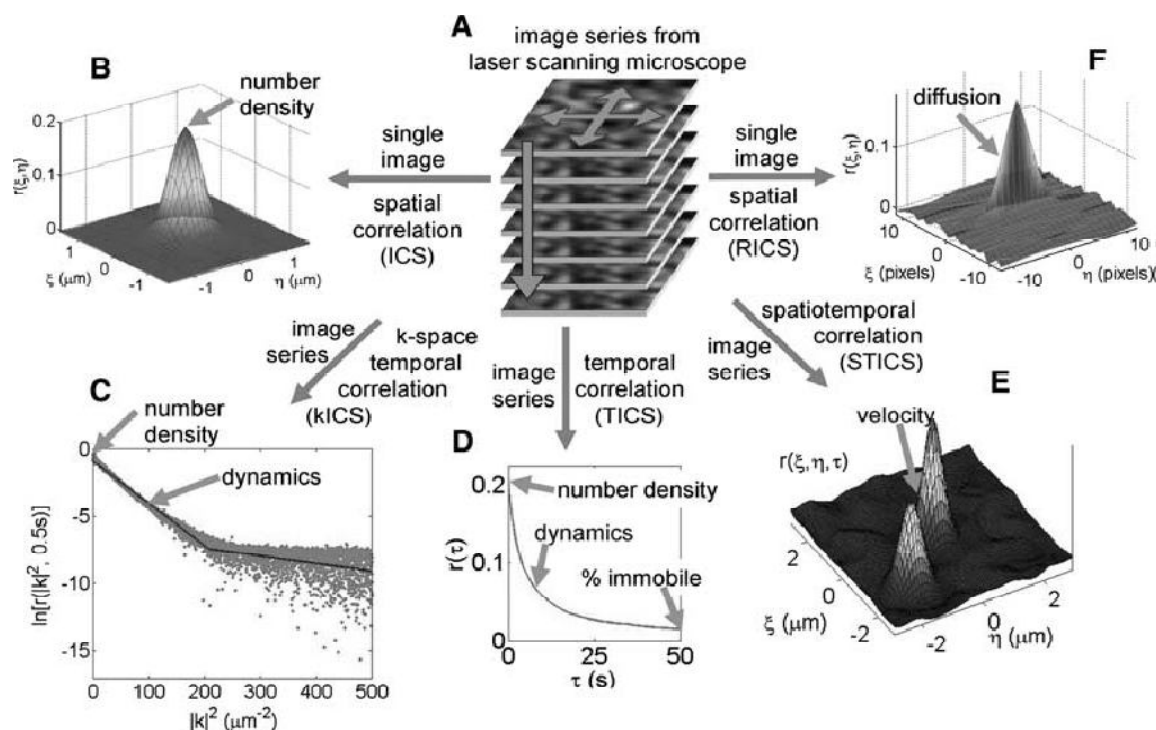


Fig. 1: An overview of the image correlation techniques. [1] (A) The data for image correlation analysis is a stack of images obtained from confocal or two-photon laser scanning microscope, or a total internal reflection fluorescence microscope where the macromolecule of interest in the sample is selectively tagged with a fluorophore. (B) ICS (C) kICS (D) TICS (E) STICS (F) RICS

Image cross-correlation spectroscopy (ICCS) is a powerful techniques used to study the interaction between different proteins [1]. Here, two different proteins of interest are attached to two fluorophores with different emission wavelength, and ICCS quantifies the coexisting spatial fluctuations of images collected in two different detection channels.

Particle Image Correlation Spectroscopy (PICS) is a hybrid technique; it contains elements of both spatiotemporal image correlation spectroscopy and single-particle tracking. It can resolve correlations in nanometer length and millisecond timescale [7]. Consequently, this process can measure high diffusion coefficients at high densities, as long as the particle of interest can be resolved by the imaging system.

Raster image correlation spectroscopy (RICS) exploits the spatial autocorrelation hidden time structure of the raster-scanned images to calculate to determine the fast transport dynamics. RICS has enabled rapid as well as slow diffusion measurement on a commercial LSM analogous to single point FCS [5]. The details of this technique are further explained in the thesis.

Each of these techniques can be applied to analyze images acquired by commercial laser scanning or total internal reflection fluorescence microscopes and are used to determine the number density, aggregation state, diffusion coefficient, velocity, and interaction



fraction of fluorescently labeled molecules or particles within the cell. In our study we consider employ the RICS analysis technique to study the HeLa cells.

## **2. RICS – RASTER IMAGE CORRELATION SPECTROSCOPY**

### **2.1 RICS – concept**

RICS was originally developed by Digman et al. (U of California, Irvine) in 2005 [8]. The fundamental idea of RICS is that, the movement of molecules causes fluorescence fluctuation at a given pixel. If the intensity at each pixel is measured for a brief time in series and a fluorescence molecules moves to the neighboring pixel, there will be a correlation in the intensity fluctuation of neighboring particles with certain time delay. This resulting spatial correlation corresponds to molecular dynamics like rate of diffusion over a broad time window [2]. Thus RICS is a combination of the temporal scales of single-point FCS and spatial information as obtained from ICS.

#### **2.1.1 The hidden time structure - effects of raster scanning**

The fluorescence intensity fluctuations between the neighboring pixels are best captured by the raster-scan facility of a line scanning microscopy (LSM) or circular scan of FCS. This technique enables data acquisition from different spatial locations at different times. For instance, in raster-scan microscopy the adjacent volumes along the scanning line are sampled very rapidly; but the adjacent volumes in two consecutive lines are sampled at a much slower rate. This difference in sampling time can be exploited to measure range of diffusion coefficients, from very fast molecular diffusion which occurs in the

microsecond range to slower diffusion, which occurs on a time scale of milliseconds to even seconds.

In case of immobile particles or particles moving very slowly, there is a superposition of PSF between adjacent points, resulting in a correlation between intensities at adjacent points. For example, consider the slow moving particle as in Fig 2b situation 1; the signal can be detected at 1, 2 and 3 but not 4. Hence, the two dimensional (2-D) spatial correlation of the particle reflects the extent of superposition of the PSF in the adjacent points. However, for fast moving particles as in Fig 2b situation 2, if the distance is less than the width of the PSF then there may be some correlation of the fluorescence resulting in a spatial correlation less than that for immobile particles. For points that are not superimposed by the PSF there may be some correlation due to diffusion of particle to these points.

Spatial correlations for small diffusing particles depend on the spatial overlap and the time interval between adjacent pixels. Random diffusion of particle and longer time intervals between data points decrease correlation at shorter spatial scales but increase correlation at distant pixels. This change in the shape of the correlation function contains information about the molecular diffusion.

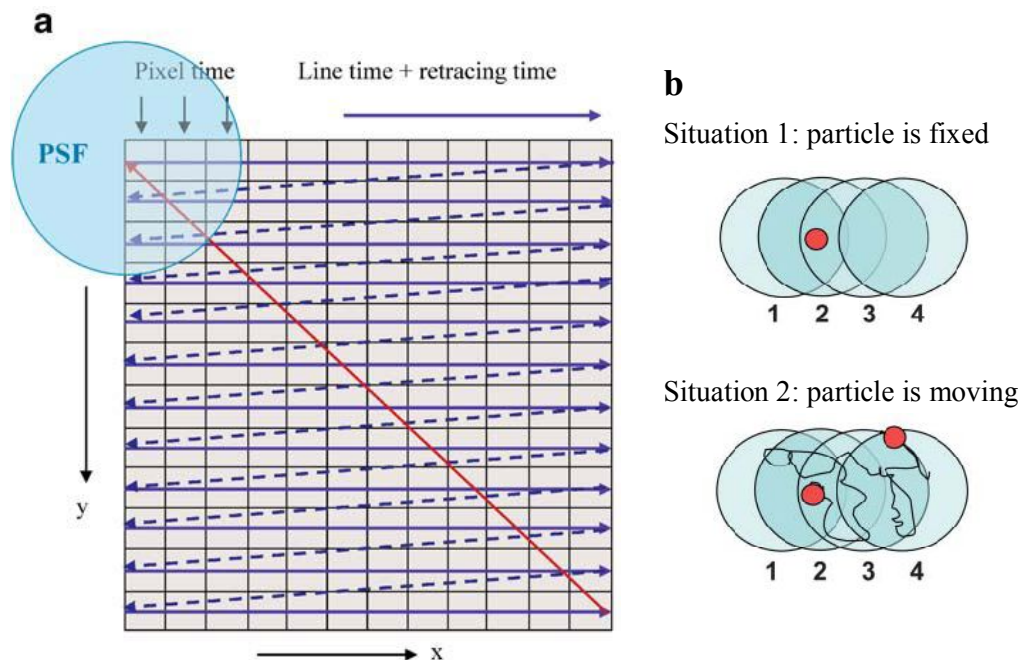


Fig. 2: RICS concept. a) Graphical representation of raster imaging [9]. Raster imaging contains temporal information as the pixels are recorded sequentially. (Situation 1) if a particle is immobile or moving slowly, signal would be detected at position 1, 2, and 3 but not at 4 during the scan. (Situation 2) if the particle diffuses quickly, it is likely to get some signal even at location 4. [8]

### 2.1.2 Subtraction of immobile features

The image stack subjected to RICS analysis, often has immobile features with dominant correlation pattern, making it difficult to see the fast diffusion particles.[5] To remove the high frequency component and effectively filter out the fixed or slow moving structures the stack of images are subjected to an immobile subtraction algorithm. The immobile feature subtraction can be done using two methods one is by subtracting average method and the other is moving average method. In subtract average method; the average image of the entire stack is subtracted from each frame. As a result the

denominator of the autocorrelation function nears zero, making it oscillate widely. Consequently, the mean of the average image is added back to each frame to avert this effect [5]. Average subtraction results in cancellation of autocorrelation due to fixed structures in 2D spatial correlation calculated.

Another method used to remove the immobile features is the moving average method. This method is used when structures within the cell are moving or the cell itself is dynamic [10]. The fast fluctuations that propagate from pixel to pixel or from line to line remain unaffected by the moving average subtraction algorithm. However, it will affect the fluctuation moving from frame to frame depending on the frame size selected. For instance, for removal of a 10 frame time window the average of frames 1–10 would be subtracted from frame 11, and the average of frames 2–11 would be subtracted from frame 12 and so on with a moving average through the entire image stack. The first 5 frames and the last five frames of the image would be ignored due to lack of enough data to perform the running average calculation properly. This eliminates the influence of cellular or sub-cellular movements longer than 10 frames in the ACF [10].

The immobile removal algorithm used can be well represented as follows [11]

$$ICS(F(x,y)) \quad \text{where} \quad F(x,y) = I(x,y) - \overline{I(x,y)} + a \quad (1)$$

where, ICS indicates the image correlation operation,  $I(x,y)$  is the intensity of frame,  $\overline{I(x,y)}$  is the average intensity of the entire frame and  $a = \overline{I(x,y)}$ . It very well represented in the Fig 3.

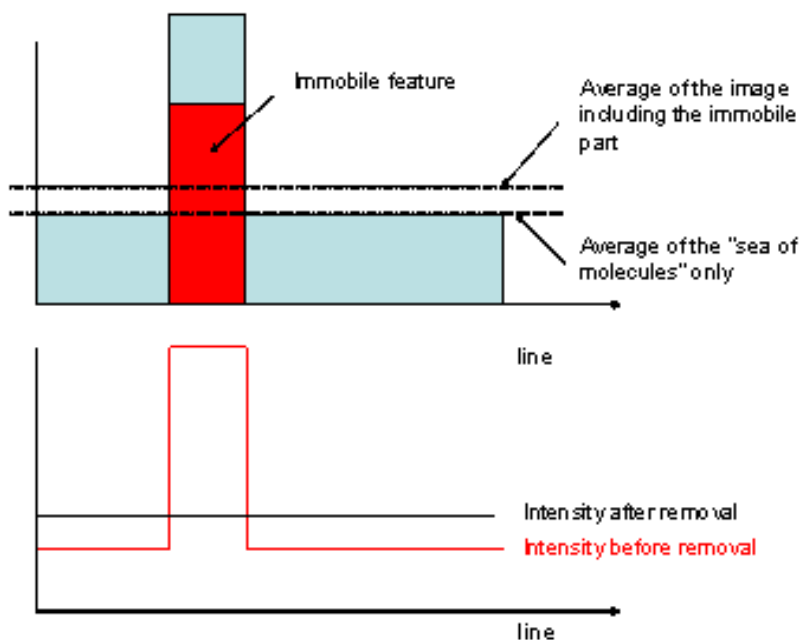


Fig. 3 : Illustration of immobile subtraction in RICS [11].

## 2.2 RICS – theory

Fluctuations in fluorescent intensity in microscope images can be caused by molecular processes such as conformational transitions, quenching associated with aggregation and molecular rotations as well as diffusion [5]. However for RICS analysis, mathematical derivations only consider signal fluctuations due to diffusion of particles in

homogeneous medium. Since, diffusion is a common mode of intercellular molecular transport. Diffusion of a particle in a homogeneous is given by the following expression,

$$C(r,t) = \frac{1}{(4\pi Dt)^{3/2}} \exp\left(-\frac{r^2}{4Dt}\right) \quad (2)$$

where  $C(r,t)$  is the concentration proportional to probability of finding a particle characterized by  $D$ , the diffusion coefficient at a position  $r$  and time  $t$  when the particles are at origin (i.e.  $r=0$ ) at time  $t=0$ . The above equation consists of a temporal part and a Gaussian. If a particle is a origin at  $t=0$ , the probability of finding the particle at a distance  $r$  from the origin is given by Gaussian distributed probability where the variance depends on time and diffusion coefficient of the particle [5].

In single-point FCS, the concentration is sampled at one position, the resulting temporal autocorrelation function of the fluorescence intensity decays with a characteristic time that depends on the diffusion coefficient and the size of the illumination volume. Instead, if the concentration is sampled at different spatial locations using a raster scan. The spatial autocorrelation function of the fluorescence decays with a characteristic length that depends on the diffusion coefficient and the size of the illumination volume [5].

### 2.2.1 Calculation of the RICS surface

Several frames (50–100) of a raster scan image acquired in rapid succession using fluorescent microscopy form the data for RICS analysis. RICS is a mathematical extension of ICS. To reveal the spatial part of the correlation function a transpose matrix is constructed from the time series of the image. For a raster scanned image the columns correspond to the points along the line, subsequently; each row corresponds to a different line. The matrix forms the pseudo-image of the raster, with time forming the vertical axis and not space. Thus the entire time series is divided into pseudo-image stacks of frames in accordance to  $2^n$  format for calculating spatial autocorrelation using fast-Fourier methods, e.g.  $256 \times 256$  [5]. This form of image representation enables the separation of spatial and temporal parts of the pseudo-image. In raster or line scan, the time series is not continuous in successive points due to line retracing; on the contrary, the image is contiguous among adjacent points. In other words, the points are equally separated in space and not in time. Hence spatial correlation is applied to the images of raster scan. The spatial correlation function is defined as follows [2],

$$G_{RICS}(\xi, \psi) = \frac{\langle I(x, y) I(x + \xi, y + \psi) \rangle}{\langle I(x, y) \rangle \langle I(x, y) \rangle} - 1 \quad (3)$$

This is called RICS autocorrelation function. Where  $I(x, y)$  is a matrix representing one image of the stack,  $\xi$  is the increment in x direction and,  $\psi$  is increment in y direction.



The angled brackets  $\langle \dots \rangle$  represent averaging over all coordinates of one image. The autocorrelation operation is schematically shown in Fig 4a. The x-axis is considered to be the fast scanning axis of the image in the derivations.

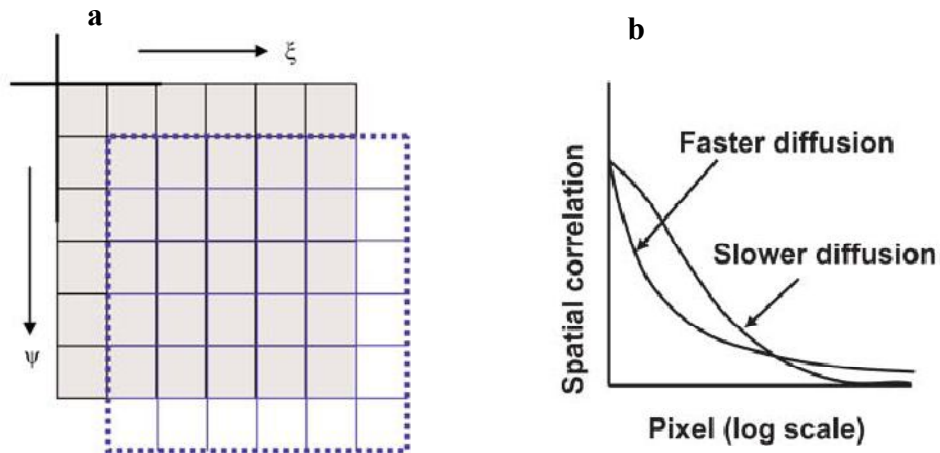


Fig. 4: a) Graphical representation of autocorrelation operation, b) The spatial extent of the correlation increases due to diffusion. [8]

### 2.2.2 RICS equations for diffusion

The RICS correlation function is written as the product of three terms. First term corresponds to the effect of diffusion and how the intensity at one pixel propagates to the next neighbor pixel. This time dependent term accounts for the difference in time between the horizontal line and the vertical line in the raster scan data acquisition method.

$$G_D(\xi, \psi) = \frac{\gamma}{N} \left( 1 + \frac{4D(\tau_p \xi + \tau_l \psi)}{\omega_0^2} \right)^{-1} \left( 1 + \frac{4D(\tau_p \xi + \tau_l \psi)}{\omega_z^2} \right)^{-1/2} \quad (4)$$

Here,  $D$  is the diffusion coefficient in units of  $\mu\text{m}^2/\text{s}$ ,  $\tau_p$  is the pixel dwell time in s,  $\tau_l$  is the line time in s, and  $\omega_0$  is the waist ( $1/e^2$ ) of the PSF in microns in the radial and  $\omega_z$  is the axial directions.  $\gamma$  is a factor that accounts for the non-uniform illumination (0.35 for 3D Gaussian, 0.076 for Gaussian Lorentzian), and  $N$  is the number of molecules in the excitation volume.

The second term of the RICS autocorrelation function describes the apparent broadening of the PSF caused by the diffusion of molecules. In the absence of diffusion, this term is just the spatial correlation of the PSF in the radial direction, described with a Gaussian. When diffusion is present, the standard deviation of this Gaussian term becomes time dependent as shown below:

$$S(\xi, \psi) = \exp \left( - \frac{\left( \frac{\delta r}{\omega_0} \right) (\xi^2 + \psi^2)}{1 + \frac{4D(\tau_p \xi + \tau_l \psi)}{\omega_0^2}} \right) \quad (5)$$

In this expression  $\delta r$  is the pixel size, in microns.

The third term accounts for the presence of blinking or any other process that changes the fluorescence intensity of the diffusing molecule. This “time” dependent part of the autocorrelation function given by the following expression [2] :

$$G_T(\xi, \psi) = 1 + A e^{-(\tau_p \xi + \tau_1 \psi) / \tau} \quad (6)$$

where A, is a constant that depends on the fraction of molecules blinking and on the difference in fluorescence intensity between the two states for pure blinking.  $\tau$  is the characteristic time period, accounts for both on and off time of fluorescence. In the above derivation, the same molecule is blinking and diffusing.

The spatial autocorrelation function for RICS is derived assuming that the intensity fluctuation due to diffusion of a particle that is small compared to the PSF. The product of the above three terms describes the overall correlation function [2], and is given by

$$G(\xi, \psi) = G_D(\xi, \psi) \cdot S(\xi, \psi) \cdot G_T(\xi, \psi) \quad (7)$$

### 2.2.3 RICS equations for binding

For a molecule undergoing binding–unbinding to a fixed location, the fluorescence will “blink”, and the diffusion time is much shorter compared to the time the molecule is

fixed at the binding site. The RICS autocorrelation function for a molecule undergoing binding–unbinding to a fixed location is given by

$$G_{\mathbf{B}}(\xi, \psi) = Ae^{-\left[\left(\frac{\xi \delta r}{\omega_0}\right)^2 + \left(\frac{\psi \delta r}{\omega_0}\right)^2\right]} e^{-(\tau_p \xi + \tau_p \psi) / \tau} \quad (8)$$

A is constant and depends on the inverse of the number of binding sites and on the “contrast” between the site to be occupied or not [2]. The time constant  $\tau$  depends on both on and off binding times.

If in a sample there are both diffusing independent molecules and molecules undergoing binding–unbinding, the overall correlation function is the linear combination of the correlation functions due to each type of molecules weighted by the square of the relative fluorescence intensity contribution.

### 2.3 RICS - method

For RICS analysis, data is collected using a confocal laser-scanning microscope. The sample is raster scanned with a pixel dwell time (order of few microseconds). The line of the scan has duration in the order millisecond and the entire frame is acquired in the order of 1s [2]. This raster scanning embeds a space-time matrix of pixels within the image. This enables measurement of fast transport dynamics over a wide dynamic range unlike FCS, which measures fluorescence fluctuation at a single spot. RICS analysis

requires oversampling of the PSF, i.e. the pixel size ( $0.05 \mu\text{s} - 0.1 \mu\text{s}$  range) has to be substantially smaller than the width of the PSF ( $0.2-0.3 \mu\text{m}$ ).

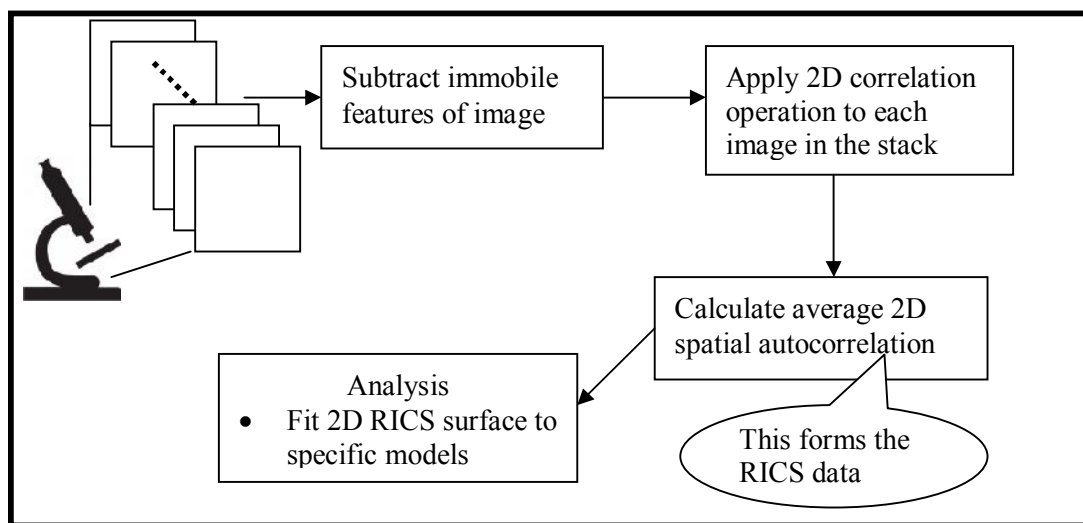


Fig. 5: Schematic of RICS method.

For the analysis the frame acquisition is repeated about 50 – 100 frames. Theoretically, one frame can give the autocorrelation function and diffusion coefficient of moving particles but in practice, the result is averaged over many frames to improve statistics. We used the SimFCS program (Laboratory for Fluorescence Dynamics) for the RICS analysis.

The data in the stack of image is processes first by removing the immobile feature in the image using the immobile subtraction algorithm. Consequently, each frame in the stack is subjected to 2D correlation operation, then; the average 2D spatial correlation is

calculated. This 2D spatial correlated data constitutes as RICS data, which is then displayed and analyzed by fitting it to specific models [2]. RICS approach exploits the time structure present in the images enabling measurements of both fast process (due to the pixel dwell time in microseconds scale) and also slow process (due to the line time in millisecond scale and frame in seconds) [2].

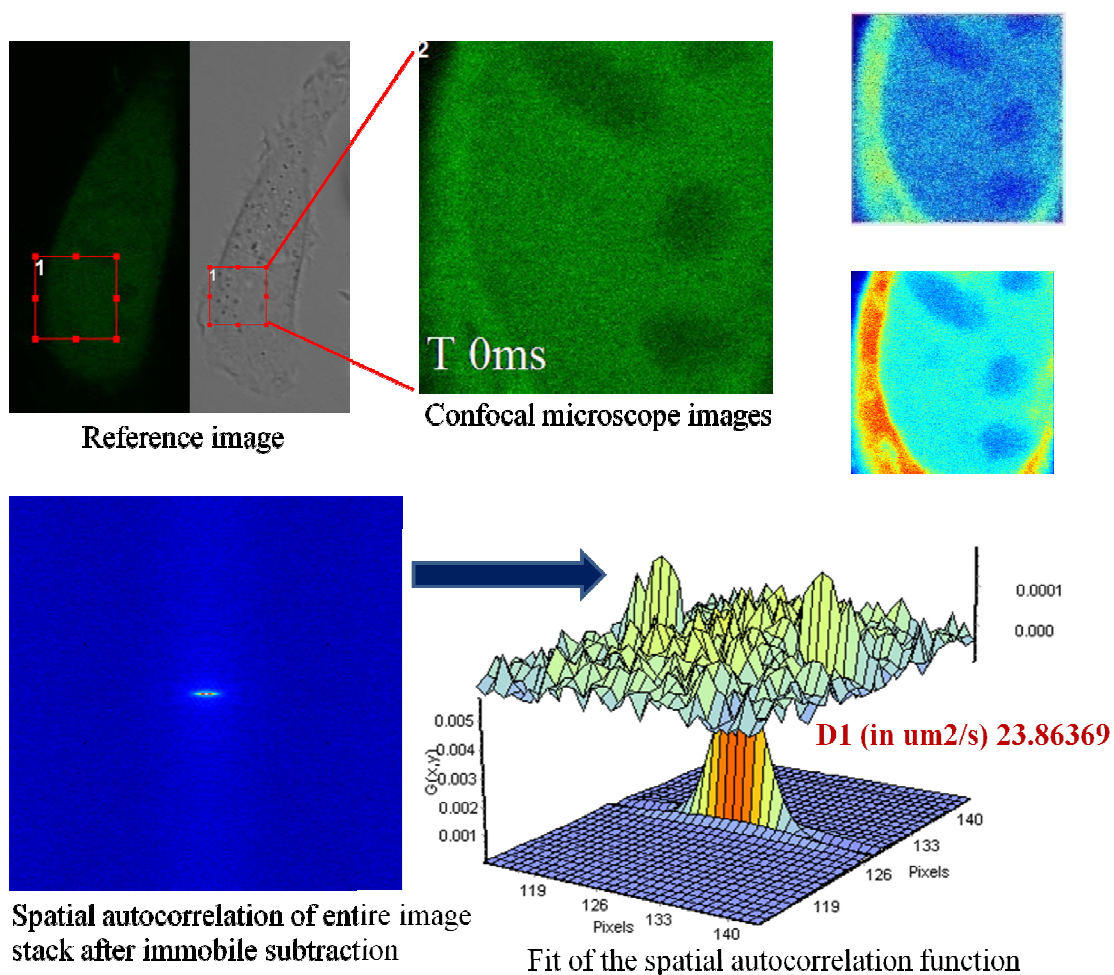


Fig. 6: RICS method example. To illustrate the RICS method a stack of 100 images of GFP-alone in HeLa cell analysis is displayed. The diffusion coefficient of GFP alone in the nucleus region of the cell is  $23.86 \mu\text{m}^2/\text{s}$ .

The effects of diffusion and binding can also be distinguished under some conditions, which depend on pixel dwell time and line time. Thus, RICS bridges the time scales of Fluorescence Correlation Spectroscopy (FCS) and ICS to resolve information in microseconds to seconds time range [8].

#### **2.4 Advantages of RICS technique**

RICS is a non invasive fluometric technique that allows imaging in vivo. The fundamental advantage of RICS is that it is analogous to confocal microscopy that is commonly used in educational institutes [8]. This novel image-analysis technique unveils the hidden dynamic information within each image collected on a LSM allowing us to study variety of cellular dynamics in time span varying from microsecond to second. “The beauty of RICS technique is that it allows one to measure the dynamics of soluble cytosolic protein, membrane associated protein, slow-moving transmembrane protein, multiprotein complex dynamics and protein binding equilibrium from a single image time series.”[5]. Importantly, it can be done even in the presence of large immobile features found in the cell. It also supports an intrinsic method to separate the immobile fraction. It can be used to study the molecular mobility over a wide area of the cell. One of the main advantages of RICS over FCS is that kinetic information can be spatially mapped allowing for the detection of heterogeneities in diffusion [12].

### **3. PROTEIN STUDY**

The protein dynamic study within the living cell can give a better insight to the underlying biology [1] by exposing the intercellular signaling pathway. Thus help clearly understand and characterize wide range of biochemical reactions that occurs within the living cells.

#### **3.1 Green Fluorescent Protein - GFP**

Green Fluorescent Protein, companion protein the chemiluminescent protein from *Aequorea* jellyfish to aequorin, was discovered by Shimomura et al [13]. Versatility of GFP to be attached to virtually any protein of interest and still fold into a fluorescent molecule has revolutionized the study of cellular behavior [14]. The fusion protein not only maintains the normal functions and localizations but also induces fluorescence. These GFP have further been engineered to improve brightness, photostability and expression properties [14]. Typically a mammalian cell is transfected with a cDNA chimera composed of a fusion of the genes encoding the fluorescent protein and protein of interest. The gene is transcribed within the nucleus to produce mRNA which is in turn translated to form the chimeric protein. This enables to learn about the trafficking and localization of the protein primarily dictated by the protein-of-interest. It facilitates minimal invasive in vivo imaging of cells thus forming an ideal candidate to study protein to protein interaction at molecular level. . Cells that express proteins tagged with



these GFPs can be imaged provide useful information about changes in the steady-state distribution of a protein over time due to high temporal and spatial resolution [13]. The fluorescent protein in conjunction with imaging tools has given invaluable insights into the behavior of proteins, organelles and cells. This ushered in a new era of cell biology in which kinetic microscopy methods can be used to decipher pathways and mechanisms of biological processes.

### **3.2 EGFR-Epidermal Growth Factor Receptor**

Epidermal growth factor receptors are bound to cell-surface receptors. They are important regulators of normal survival and cell proliferation. There are four known human epidermal growth factor receptors (HER) [15]. An external ligand or the growth factor molecule initiates dimerization of the receptors on the cell membrane. This in turn activates intercellular signaling proteins to perform a series of process for cell survival or cell proliferation [15]. Disregulation in these signal transduction pathways, results in overexpression of growth factor receptors that would increase the signal transduction consequently increase in activation of transcription leading to the growth and progression of many solid tumors [16]. These EGFR can also be one of the reasons for metastasis of cancer [15]. Thus regulating EGFR cell signaling can be an anticancer strategy. Hence we study GFP-EGFR fusion protein transfected into the HeLa cells without any treatment to observe the diffusion coefficient.

### 3.3 p53

For our experiments the protein of interest is p53 also known as the “guardian of the genome”, "the guardian angel gene", and the "master watchman" [17]. This protein is conserved stability by preventing genome mutation. In a normal cell p53 protein is in the switched off state as it is capped with another protein called MDM2. When the cell detects DNA damage p53 protein is activated. The p53 in activated state either arrest the cell cycle and repairs the DNA and resumes the cell cycle or initiates cell signaling for cell apoptosis thus helps maintain cellular and genetic stability. However in many cancers, this protective activity is switched off due to over expression of the protein MDM2, which blocks p53 [17]. Inhibiting the binding of MDM2 has been suggested as an anticancer strategy. In our experiment we try to determine the diffusion coefficient of p53 in HeLa cells using the RICS technique to understand the trafficking and signaling pathways of p53 in the cervical cancer cells.

## **4. MATERIALS AND METHODS**

### **4.1 Cell culture and protein transfection**

HeLa cells for the experiments were provided by Dr. M. C. Hung (M.D. Anderson Cancer Center, TX). Cells were transfected with p53 fused with the green fluorescent protein (GFP), GFP-EGFR, GFP-p53 or GFP alone as a control using electroporation. After plating the transfected cells on glass bottom culture dishes of 0.17 mm thickness (MatTek Corporation). For GFP-p53 and GFP alone cells were either treated with 20  $\mu$ M cisplatin (Sigma) or 20 nM etoposide (Sigma) or left untreated for 12 hr and then analyzed using confocal microscopy. For GFP-EGFR the cells are left untreated.

### **4.2 Microscopy specifications**

We used an Olympus FV1000 microscope with a 60 $\times$  1.2 NA water objective (Olympus, Tokyo, Japan). The scan speed was set at 12.5 seconds per pixel. The scan area was 256  $\times$  256 pixels and about 100 frames were collected for each sample. The corresponding line time was calculated as 4.35 ms and the frame time was 1.114 s. The electronic zoom of the microscope was set to 4.1, which corresponds to a region of 12.5  $\mu$ m square. For the GFP excitation, we used the 488 nm line of the argon ion laser. The power of the 488 nm laser was set between 1.5% according to the power slider in the FV1000 microscope. Data was collected in the pseudo photon counting mode of the Olympus FV1000

microscope. The filter for the green emission channel had a nominal bandwidth of 500–600 nm. The beam waist radius was estimated from the Airy disk projected from the objective into the specimen (= twice the optical resolution of the objective).

$\text{Airy} = (1.22 \times \text{wavelength of the signal}) / \text{Numerical aperture of the objective}$

Thus,  $1.22 \times 0.488 / 1.2 = 0.488 \mu\text{m}$  is beam waist diameter. The radius is then  $\sim 0.2 \mu\text{m}$ .

## 5. RESULTS

Our proteins of interest are GFP-EGFR and GFP-p53. We observe the diffusion coefficient in HeLa cells transfected with GFP-EGFR without any treatment administered to the cells. To study p53 diffusion coefficient the cells are observed in three conditions; one set of HeLa cells are treated with cisplatin, second set treated with etoposide and the third set is left untreated. The above mentioned conditions are also administered with GFP-alone to act as a control to the experiment. Cisplatin and etoposide are drugs given to damage the DNA. Cisplatin denatures the DNA strands form double strand to single strands whereas etoposide cuts the DNA double strands into pieces.

For the RICS analysis data were collected using confocal microscope in pseudo photon counting mode in the  $256 \times 256$  frame format. For each sample, data was collected separately for nucleus and cytoplasm for three cells. The regions of interest (ROIs) for RICS analysis were selected on the basis of apparent homogeneity and were taken at some distance from the cell borders. All the analysis was done using the SimFCS program (Laboratory for Fluorescence Dynamics).

Measuring diffusion in live cells is challenging as they often contain many immobile features like adhesions, edges, organelles etc. which give high spatially correlation that dominate the ACF. Hence to prevent the loss of potential useful information the image

stack is subjected to the immobile features removal algorithm. We also observe that the cell organelles move during image acquisition, therefore, subtracting an average of all frames within the movie will result in a broadening of the ACF. This broadening is due to the fact that the movements of adhesions within the cell prevent complete removal of the immobile components. Therefore we subject the stack of images to a 10 frame moving average immobile removal algorithm as described before. The software calculates and displays the spatial correlation average. The data is then displayed and analyzed by fitting it in a 3D diffusion models.

Five  $128 \times 128$  ROIs were analyzed for diffusion for each  $256 \times 256$  image series. For clarity, only one of the five ROIs is shown in Figs. 7-13. The diffusion coefficient of GFP-EGFR was determined to be  $0.0275 \pm 0.0288 \mu\text{m}^2/\text{s}$  in nucleus and  $0.237 \pm 0.151 \mu\text{m}^2/\text{s}$  in cytoplasm. The average diffusion coefficient of GFP-p53 and GFP-alone for both treated and non treated condition is tabulated in Table 1 for clarity.

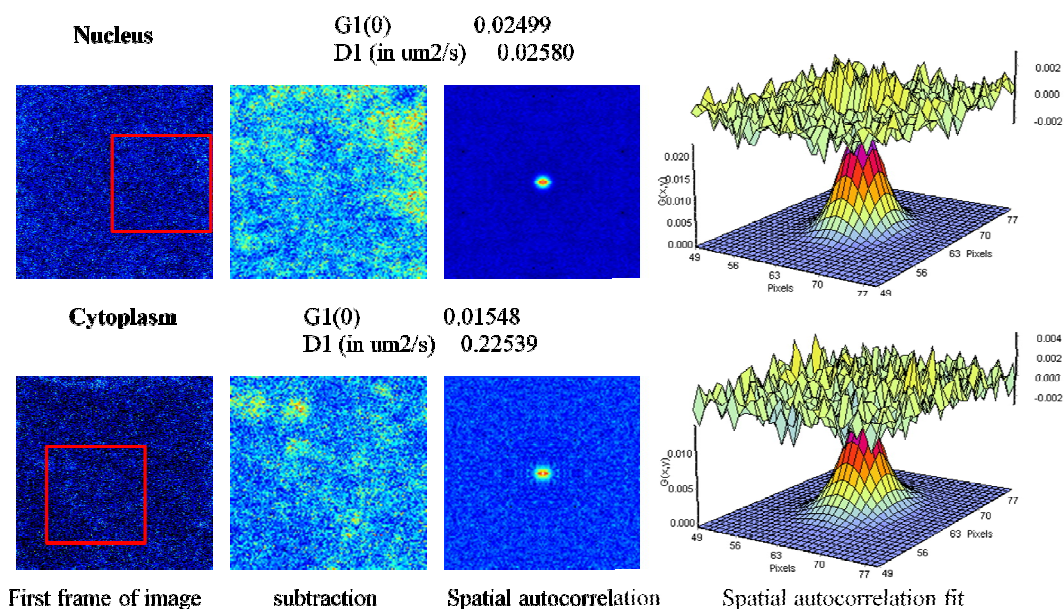


Fig. 7: RICS analysis of GFP- EGFR in HeLa cells. The diffusion coefficient was determined to be  $0.0275 \pm 0.0288 \mu\text{m}^2/\text{s}$  in nucleus and  $0.237 \pm 0.151 \mu\text{m}^2/\text{s}$  in cytoplasm

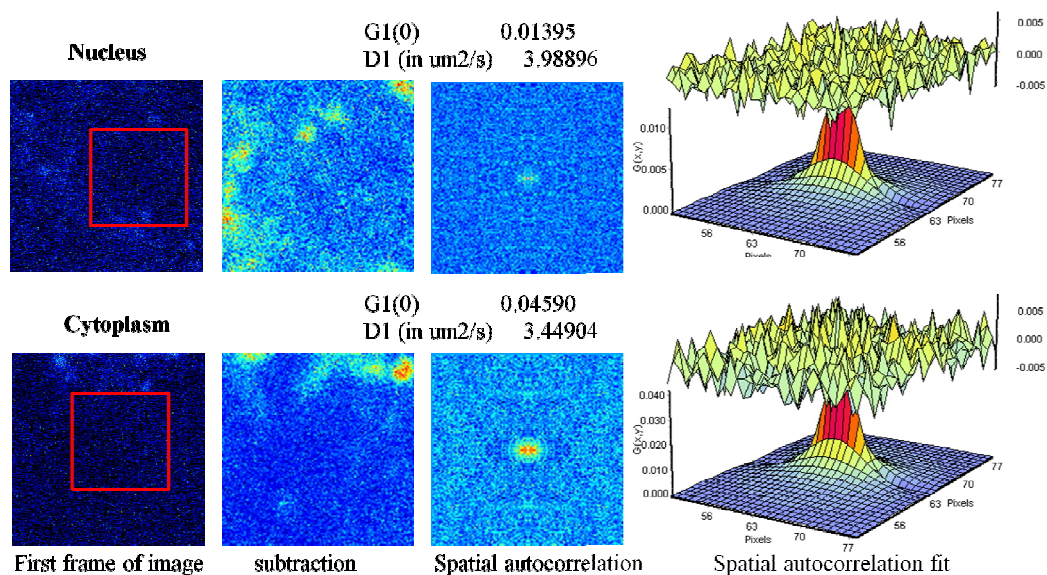


Fig. 8.: RICS analysis of GFP- P53 without treatment in HeLa cells. The diffusion coefficient was determined to be  $10.07 \pm 5.25 \mu\text{m}^2/\text{s}$  in nucleus and  $17.03 \pm 5.2 \mu\text{m}^2/\text{s}$  in cytoplasm

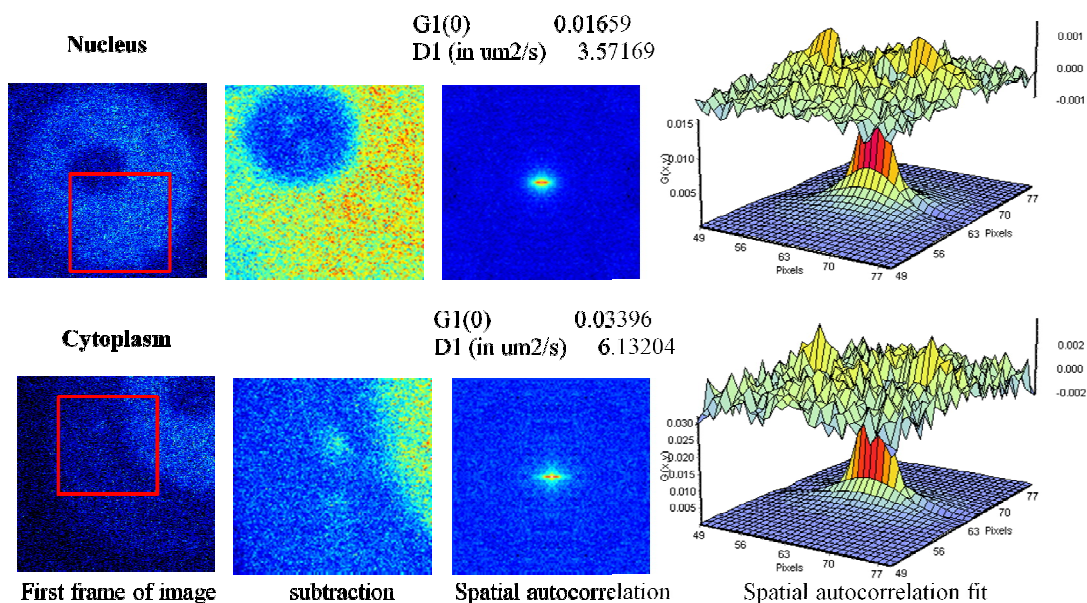


Fig. 9: RICS analysis of GFP- P53 with cisplatin treatment in HeLa cells. The diffusion coefficient was determined to be  $3.26 \pm 0.73 \mu\text{m}^2/\text{s}$  in nucleus and  $7.02 \pm 2.93 \mu\text{m}^2/\text{s}$  in cytoplasm

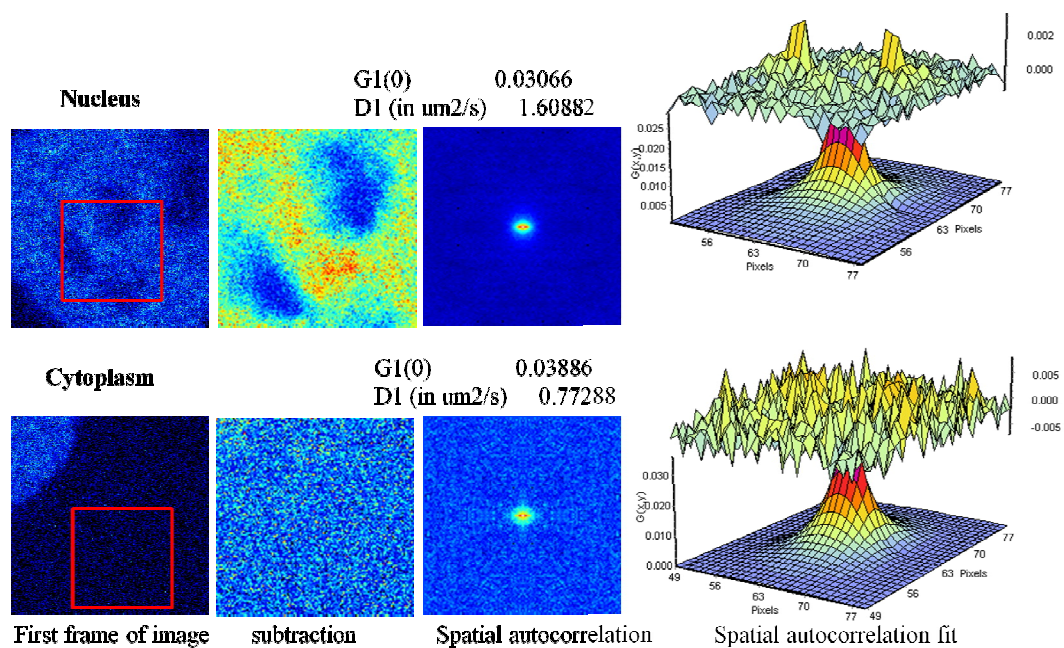


Fig. 10: RICS analysis of GFP- P53 with etoposide treatment in HeLa cells. The diffusion coefficient was determined to be  $1.72 \pm 0.275 \mu\text{m}^2/\text{s}$  in nucleus and  $1.279 \pm 1.29 \mu\text{m}^2/\text{s}$  in cytoplasm.



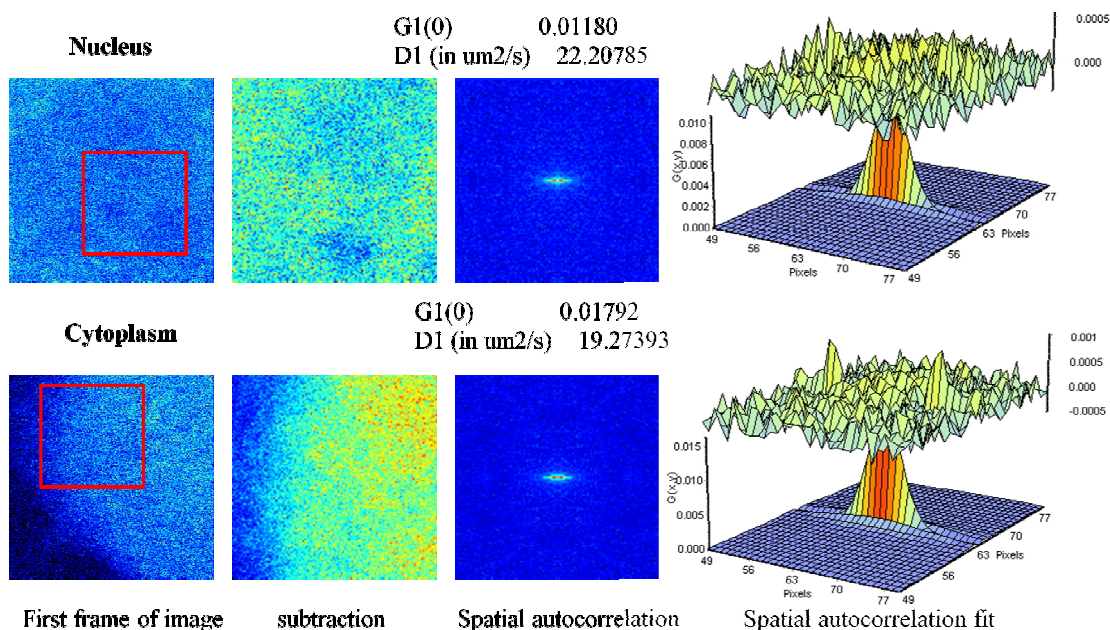


Fig. 11: RICS analysis of GFP- alone with no treatment in HeLa cells. The diffusion coefficient was determined to be  $19.14 \pm 2.87 \mu\text{m}^2/\text{s}$  in nucleus and  $16.17 \pm 1.675 \mu\text{m}^2/\text{s}$  in cytoplasm

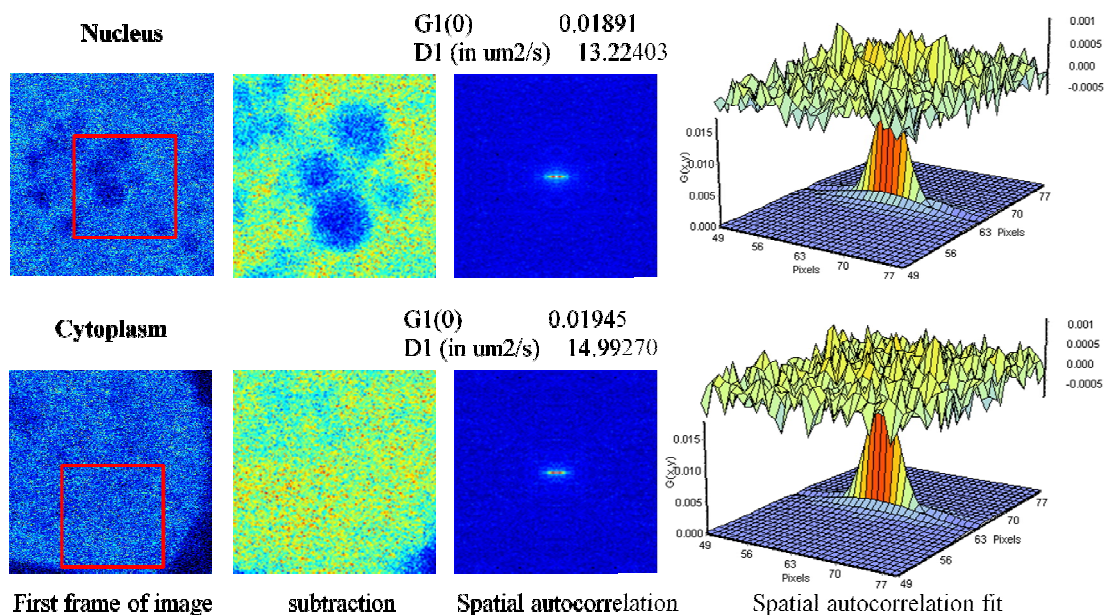


Fig. 12: RICS analysis of GFP- alone with cisplatin treatment in HeLa cells. The diffusion coefficient was determined to be  $17.37 \pm 3.1 \mu\text{m}^2/\text{s}$  in nucleus and  $19.24 \pm 3.03 \mu\text{m}^2/\text{s}$  in cytoplasm

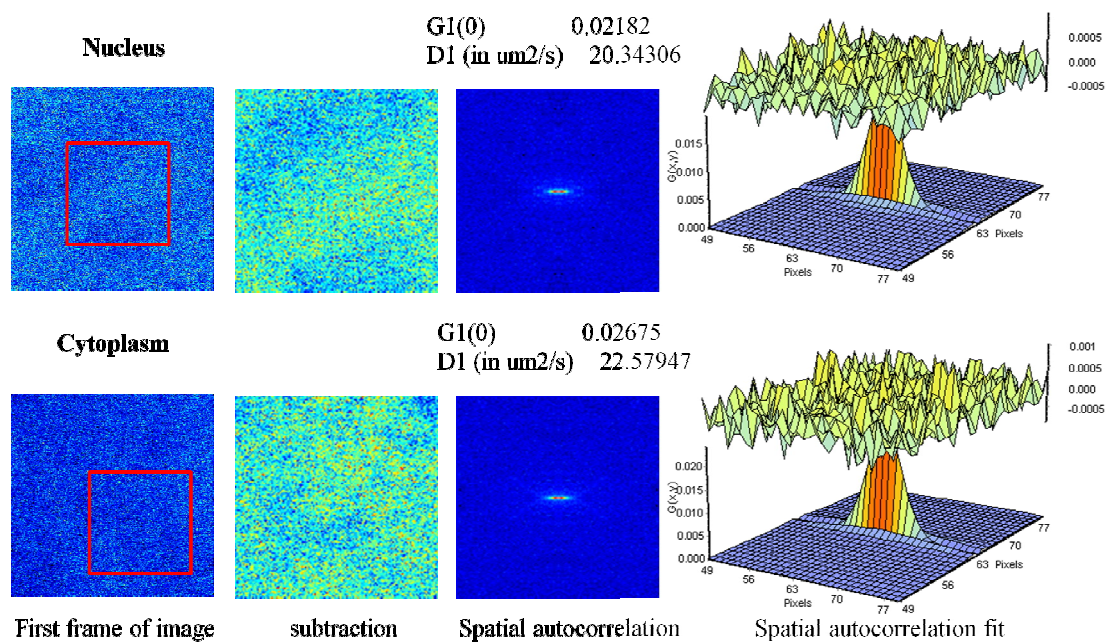


Fig. 13: RICS analysis of GFP- alone with etoposide treatment in HeLa cells. The diffusion coefficient was determined to be  $21.47 \pm 2 \mu\text{m}^2/\text{s}$  in nucleus and  $20.94 \pm 2.87 \mu\text{m}^2/\text{s}$  in cytoplasm

TABLE I  
 COMPARISON OF DIFFUSION COEFFICIENTS OF GFP-P53 AND GFP –ALONE IN HELA CELLS FOR DIFFERENT CONDITIONS

GFP-p53 without treatment			GFP-alone without treatment		
	D ( $\mu\text{m}^2/\text{s}$ )	$\sigma$		D ( $\mu\text{m}^2/\text{s}$ )	$\sigma$
Nucleus	10.07224	5.245964	Nucleus	19.143699	2.87188018
Cytoplasm	17.02946	5.216444	Cytoplasm	16.171526	1.67532826
GFP-p53 with cisplatin treatment			GFP- alone with cisplatin treatment		
	D ( $\mu\text{m}^2/\text{s}$ )	$\sigma$		D ( $\mu\text{m}^2/\text{s}$ )	$\sigma$
Nucleus	3.2621847	0.72739116	Nucleus	17.368559	3.10087845
Cytoplasm	7.016822	2.93046996	Cytoplasm	19.240561	3.0332588
GFP-p53 with etoposide treatment			GFP- alone with etoposide treatment		
	D ( $\mu\text{m}^2/\text{s}$ )	$\sigma$		D ( $\mu\text{m}^2/\text{s}$ )	$\sigma$
Nucleus	1.714976	0.27491466	Nucleus	21.467979	2.0018405
Cytoplasm	1.269142	1.29078985	Cytoplasm	20.938131	2.867562

D = diffusion coefficient ,  $\sigma$  = Standard Deviation, m = meter

## 6. DISCUSSION AND CONCLUSION

### 6.1 Discussion

In this paper, we described the implementation of RICS on Olympus confocal microscope with photon counting mode to determine diffusion of coefficient of our protein of interest GFP-EGFR and GFP-p53 in HeLa cells under different conditions.

The diffusion coefficient of GFP-EGFR in HeLa cells determined from the analysis was  $0.0275 \pm 0.0288 \mu\text{m}^2/\text{s}$  in the nucleus and  $0.237 \pm 0.151 \mu\text{m}^2/\text{s}$  in the cytoplasm.

The diffusion coefficient of GFP-p53 treated with cisplatin was observed to be  $3.26 \pm 0.727 \mu\text{m}^2/\text{s}$  in the nucleus and  $7.02 \pm 2.93 \mu\text{m}^2/\text{s}$  in the cytoplasm; whereas, diffusion coefficient of GFP-alone with cisplatin was observed to be  $17.37 \pm 3.1 \mu\text{m}^2/\text{s}$  and  $19.24 \pm 3.03 \mu\text{m}^2/\text{s}$  in nucleus and cytoplasm respectively. Furthermore, the diffusion coefficient of GFP-p53 treated with etoposide was observed to be  $1.72 \pm 0.275 \mu\text{m}^2/\text{s}$  in the nucleus and  $1.279 \pm 1.29 \mu\text{m}^2/\text{s}$  in the cytoplasm; and its corresponding GFP-alone control had a diffusion coefficient of  $21.47 \pm 2 \mu\text{m}^2/\text{s}$  and  $20.94 \pm 2.87 \mu\text{m}^2/\text{s}$  in nucleus and cytoplasm respectively. A significant decrease is observed in the diffusion coefficient of GFP-p53 in cells treated with cisplatin and etoposide compared to GFP-alone. Also from the images we observe more aggregation in the nucleus indicating the

possibility of binding of p53 and the damaged DNA resulting in reduced diffusion coefficient.

We also observe some vertical component in the average spatial correlation function as shown in Fig.14. This could indicate it some type of binding activity other than diffusion happening in the nucleus of HeLa cells treated with cisplatin and etoposide which is not accounted for by the software.

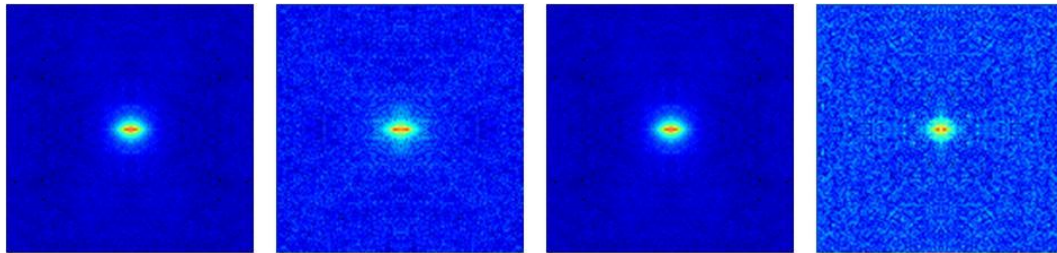


Fig. 14: 2D spatial correlation as observed in the nucleus of the HeLa cells treated with DNA damage drugs. a) and b) spatial correlation observed in HeLa cells with cisplatin treatment c) and d) spatial correlation observed in HeLa cells with etoposide treatment. The figure shows a vertical component which shows there is some binding activity other than diffusion

The value of diffusion coefficient found in literature is as follows. Diffusion coefficient of EGFR reported using FRAP or SPT the ranged around  $0.02 \mu\text{m}^2/\text{s}$  [18]. In H1299 human large cell lung carcinoma cell, the diffusion constant of p53-GFP was estimated to be  $D_{\text{p53-GFP}} = 15.4 \mu\text{m}^2\text{s}^{-1}$  which was significantly slower compared to and that of GFP-alone,  $D_{\text{GFP}} = 41.6 \mu\text{m}^2\text{s}^{-1}$  [19]. Diffusion coefficient of GFP alone in HeLa cell cytoplasm was observed to be  $24 \pm 2 \mu\text{m}^2/\text{s}$  using FRAP [20].

The detector autocorrelation time imposes an upper limit onto the diffusion coefficient that can be measured. The determination of fast diffusion requires high scan speeds, leading to increased spatial correlation induced by the detector. The detector electronics does not have enough time to reset itself before collecting the next data point. As a result, the residual signal from the previous data point will be correlated with the signal from the following data point. It is important to eliminate these bleed-through noise data points before fitting the spatial ACF since they can result in a lack of convergence of the fitting functions [3].

Among all the GFP-p53 transfected cells it was observed that only 20% to 30% express the protein giving very weak signal. The RICS technique requires higher signal to noise ratio signal to calculate the spatial correlation. Also all cells exhibit some auto-fluorescence which could also influence the correlation.

## **6.2 Conclusion**

RICS is a non-invasive fluorimetric technique that can be used to study cellular processes in conjunction with any standard laser-scanning microscope found in all life science institutions. We have successfully used this technique to determine the diffusion coefficient of three proteins GFP-alone, GFP-EGFR and GFP-p53 in human cervical cancer cells. The diffusion coefficient of GFP-EGFR was very close to the values found in the literature. Also a significant decrease in diffusion coefficient of GFP-p53

compared to GFP-alone was observed, which could explain the binding of p53 to the denatured DNA.

RICS provides a fundamental insight in the quantitative dynamics and is still in stage of infancy and the current implementation of RICS does not compensate for all types of binding observed in a cell. Further exploration with respect to the protein study is required with different drug-induced modification of intracellular structures to understand the signaling pathway. Also the next step could adapt for analysis of not only the diffusion coefficient but also to understand the increased aggregation of GFP-p53 observed in the nucleus of the treated cells.

As the technique of correlation spectroscopy are continuously improving, it should be possible, to map the underlying quantitative dynamics of the cells. This information could reveal the intercellular interactions at molecular level thus leading not only to a better understanding of diseases like cancer and diabetes but also help develop early diagnostic devices and potential treatment for the same.

### **6.3 Support and recognition**

The use of the Microscopy and Imaging Center facility at Texas A&M University is acknowledged. The Olympus FV1000 confocal microscope acquisition was supported by the Office of the Vice President for Research at Texas A&M University.

The fluorescence data were analyzed using the Globals software package developed at the Laboratory for Fluorescence Dynamics at the University of Illinois at Urbana-Champaign.

## REFERENCES

- [1] D. L. Kolin, and P. W. Wiseman, "Advances in image correlation spectroscopy: measuring number densities, aggregation states, and dynamics of fluorescently labeled macromolecules in cells," *Cell Biochemistry and Biophysics*, vol. 49, no. 3, pp. 141-164, 2007.
- [2] M. A. Digman, and E. Gratton, "Analysis of diffusion and binding in cells using the RICS approach," *Microscopy Research and Technique*, vol. 72, no. 4, pp. 323-332, 2009.
- [3] E. Gielen, N. Smisdom, M. vandeVen, B. De Clercq, E. Gratton *et al.* "Measuring diffusion of lipid-like probes in artificial and natural membranes by raster image correlation spectroscopy (RICS): Use of a Commercial Laser-Scanning Microscope with Analog Detection," *Langmuir*, vol. 25, no. 9, pp. 5209-5218, 2009.
- [4] N. O. Petersen, P. L. Hoddellius, P. W. Wiseman, O. Seger and K. E. Magnusson, "Quantitation of membrane receptor distributions by image correlation spectroscopy: concept and application," *Biophysical Journal*, vol. 65, no. 3, pp. 1135 - 1146, 1993.
- [5] M. A. Digman, C. M. Brown, P. Sengupta, P. W. Wiseman, A. R. Horwitz *et al.*, "Measuring fast dynamics in solutions and cells with a laser scanning microscope," *Biophysical Journal*, vol. 89, no. 2, pp. 1317-1327, 2005.
- [6] D. L. Kolin, D. Ronis, and P. W. Wiseman, "k-Space image correlation spectroscopy: A method for accurate transport measurements independent of fluorophore photophysics," *Biophysical Journal*, vol. 91, no. 8, pp. 3061-3075, 2006.
- [7] S. Semrau, and T. Schmidt, "Particle image correlation spectroscopy (PICS): Retrieving Nanometer-Scale Correlations from High-Density Single-Molecule Position Data," *Biophysical Journal*, vol. 92, no. 2, pp. 613-621, 2007.
- [8] M. A. Digman, P. Sengupta, P. W. Wiseman, C. M. Brown, A. R. Horwitz *et al.*, "Fluctuation correlation spectroscopy with a laser-scanning microscope: Exploiting the hidden time structure," *Biophysical Journal*, vol. 88, no. 5, pp. L33-L36, 2005.



- [9] E. Gielen, N. Smisdom, B. D. Clercq, M. vandeVen, R. Gijssbers, Z. Debyser *et al.*, “Diffusion of myelin oligodendrocyte glycoprotein in living OLN-93 cells investigated by Raster-scanning image correlation spectroscopy (RICS),” *Journal of Fluorescence*, vol. 18, no. 5, pp. 813 - 819, 2008.
- [10] C. M. Brown, R. B. Dalal, B. Hebert, M. A. Digman, A. R. Horwitz *et al.*, “Raster image correlation spectroscopy (RICS) for measuring fast protein dynamics and concentrations with a commercial laser scanning confocal microscope,” *Journal of Microscopy*, vol. 229, no. 1, pp. 78-91, 2008.
- [11] E. Gratton. “Tutorial 2 - Immobile Subtraction in RICS, ” 2009; <http://simfcs.pbworks.com/Tutorial-2>, June 2009.
- [12] M. A. Digman, C. M. Brown, A. R. Horwitz, W. W. Mantulin and E. Gratton, “Paxillin dynamics measured during adhesion assembly and disassembly by correlation spectroscopy,” *Biophysical Journal*, vol. 94, no. 7, pp. 2819-2831, 2008.
- [13] R. Y. Tsien, “The green fluorescent protein,” *Annual Review of Biochemistry*, vol. 67, no. 1, pp. 509-544, 1998.
- [14] J. Lippincott-Schwartz, N. Altan-Bonnet, and G. H. Patterson, “Review: Photobleaching and photoactivation: following protein dynamics in living cells,” *Nature Cell Biology*, vol. 5, pp. S7–S14, 2003.
- [15] D. Hanahan, and R. A. Weinberg, “The hallmarks of cancer,” *Cell*, vol. 100, no. 1, pp. 57-70, 2000.
- [16] J. Short, “Signal Transduction and Oncogene,” 2004; <http://cred.mdanderson.org/surp/resources/Oncogenes.pdf>, June 2009.
- [17] R. Serpi, “Mechanism of benzo(a)pyrene-induced accumulation of p53 tumour suppressor protein in mouse,” Academic Dissertation, Department of Pharmacology and Toxicology, University of Oulu Oulu, Finland, 2003.
- [18] G. Orr, D. Hu, S. Özçelik, L. K. Opresko, H. Steven Wiley *et al.*, “Cholesterol dictates the freedom of EGF receptors and HER2 in the plane of the membrane,” *Biophysical Journal*, vol. 89, no. 2, pp. 1362-1373, 2005.
- [19] P. Hinow, C. E. Rogers, C. E. Barbieri, J. A. Pietenpol and A. K. Kenworthy, “The DNA binding activity of p53 displays reaction-diffusion kinetics,” *Biophysical Journal*, pp. 330 - 342, 2006.

- [20] E. O. Potma, W. P. d. Boeij, L. Bosgraaf, J. Roelofs, P. J. M. van Haastert *et al.*, “Reduced protein diffusion rate by cytoskeleton in vegetative and polarized dictyostelium cells,” *Biophysical Journal*, vol. 81, no. 4, pp. 2010-2019, 2001.

## VITA

Name: Harini Bytaraya Sreenivasappa

Address: Department of Electrical and Computer Engineering  
c/o Dr. Jun Kameoka  
Texas A&M University  
College Station TX 77843-3128  
USA

Email Address: [harinibs@tamu.edu](mailto:harinibs@tamu.edu)

Education: B.E., Electronics and Communication, Atria Institute of Technology  
affiliated to Visvesvaraya Technological University, 2005  
M.S., Electrical Engineering, Texas A&M University, 2009.